PAPER

Check for updates

A phosphite derivative with stronger HF elimination ability as an additive for Li-rich based lithium-ion batteries at elevated temperatures†

Xiangzhen Zheng,[a] Tao Huang,[a] Ying Pan,[a] Yongwei Chen,[a] Mingdeng Wei [iD] *[b] and Maoxiang Wu [iD] *[a]

Phosphite derivatives as film forming additives can effectively improve the electrochemical performance of cathodes in Li-ion batteries (LIBs). In this work, ethyl bis(trimethylsilyl) phosphite (TMSPE), which contains trimethylsilyl and ethyl functional groups, is used as a P-based additive for improving the electrochemical performance of a $Li_{1.144}Ni_{0.136}Co_{0.136}Mn_{0.544}O_2$ cathode. Further, the comparative evaluation of tris(trimethylsilyl) phosphite (TMSPi), TMSPE, and triethyl phosphite (TEP) as phosphite-based additives for $Li_{1.144}Ni_{0.136}Co_{0.136}Mn_{0.544}O_2$/Li cells at 45 °C under a high voltage is also presented. Theoretical calculations and surface characterization revealed that TMSPE formed a thinner and stable cathode electrolyte interphase (CEI) on the surface of $Li_{1.144}Ni_{0.136}Co_{0.136}Mn_{0.544}O_2$, which has lower interfacial impedance, stronger HF elimination, and transition metal dissolution inhibition, resulting in the best cell performance among the three phosphite-based additives.

1 Introduction

Electrolytes play an important role in lithium-ion batteries (LIBs) and influence the application of high-energy density materials,[1] and contain solvents, lithium salts, and additives.[2–4] With the development of high-energy density LIBs, the demand for electrolytes is becoming higher. Conventional carbonated-based electrolytes decomposed more seriously when high-energy density cathode materials operated at high voltage and caused worse performance of LIBs. Therefore, electrolyte optimization has been proposed as one of the most effective ways to improve the performance of LIBs using high-energy density materials.[5,6] As a component of electrolytes, the use of additives has been widely regarded as one of the efficient routes for improving the electrochemical performance of LIBs.[7,8]

To resolve the problems for the application of high-energy density materials, a series of additives have been designed and adopted for improving electrolytes when high-energy density materials are applied in LIBs, including S-based additives,[9,10] P-based additives,[11–13] B-based additives,[14,15]

and so on. Among them, P-based additives have attracted much attention due to their extensive applications as film additives,[16–20] flame retardant additives,[21,22] and overcharge protection additives.[23] Wang *et al.* used tris(trimethylsilyl) phosphate (TMSP) as an effective additive to improve the cycling performance of a lithium-rich cathode material $Li[Li_{0.2}Ni_{0.13}Mn_{0.54}Co_{0.13}]O_2$ at 2.0–4.8 V.[16] Liu *et al.* found that (ethoxy)pentafluorocyclotriphosphazene $(N_3P_3F_5OCH_2CH_3, PFPN)$ can be used as a novel flame-retarding additive for LIBs.[21] Wu *et al.* reported that (4-methoxy)-phenoxy pentafluorocyclotriphosphazene (4-MPPFPP) can act as a novel flame retardant and overcharge protection additive for LIBs.[23] In fact, TMSP has been applied on a few high-energy density cathodes in P-based additives, such as NCM, $LiNi_{0.5}Mn_{1.5}O_2$, Li-rich cathodes, and so on.[16,19,20,24,25] Tris(trimethylsilyl) phosphite (TMSPi) has been proven more effective than TMSP as an electrolyte additive for the cyclic stability improvement of $LiNi_{1/3}Co_{1/3}Mn_{1/3}O_2$ at 4.5 V.[26] Trimethyl phosphite (TMP) and triethyl phosphite (TEP) have also been used as an additive to improve the performance of high-energy density cathodes.[27,28] However, phosphite which contains trimethylsilyl and alkyl has not been reported as an additive for high-energy density materials.

Li-rich materials, as one class of the high-energy materials, have attracted much attention due to their high specific capacity (>250 mA h g^{-1}), low cost and environmental friendliness.[29,30] However, the poor cycling performance limits their applications.[31,32] In the Li-rich based cell system, voltage decay, transition metal ion dissolution, and side

[a] *Key Laboratory of Optoelectronic Materials Chemistry and Physics, Fujian Institute of Research on the Structure of Matter, Chinese Academy of Sciences, Fuzhou 350002, P. R. China. E-mail: mxwu@fjirsm.ac.cn*
[b] *Fujian Provincial Key Laboratory of Electrochemical Energy Storage Materials, Fuzhou University, Fuzhou 350002, P. R. China. E-mail: wei-mingdeng@fzu.edu.cn*
† Electronic supplementary information (ESI) available. See DOI: https://doi.org/10.1039/d4lf00326h

© 2025 The Author(s). Published by the Royal Society of Chemistry

RSC Appl. Interfaces, 2025, **2**, 251–260 | **251**

reactions with the electrolyte have caused poor cycling performance, which become worse with increased cycling, especially at a high temperature.[33] Therefore, surface modification[34,35] and functional additive usage[16,18,28,36,37] have been proven to be effective ways for improving the performance of Li-rich based LIBs at elevated temperatures.

In the present work, ethyl bis(trimethylsilyl) phosphite (TMSPE) was investigated as an additive for improving the performance of Li-rich materials at 45 °C. Moreover, the effects of TMSPE on the performance of cells were systematically explored by electrochemical impedance spectroscopy (EIS), X-ray photoelectron spectroscopy (XPS), inductively coupled plasma-mass spectroscopy (ICP-MS), nuclear magnetic resonance (NMR) and scanning electron microscopy (SEM). A comparative evaluation of TMSPi, TMSPE and TEP is also proposed.

2 Experimental section

2.1 Preparation of electrolytes and electrodes

1.0 M $LiPF_6$ electrolytes (EC/DMC/EMC, wt%, 1:1:1) and additives (TMSP (99.9%), TMSPi (98%), TMSPE (98%), TEP (98%)) were purchased from Dongguan Shanshan Battery Materials Co., Ltd. (China) and Fujian Shaowu Chuangxin New Materials Co., Ltd. (China), respectively. The electrolytes with additives were prepared in an argon-filled glove box (H_2O and $O_2 \leq 1$ ppm). $Li_{1.144}Ni_{0.136}Co_{0.136}Mn_{0.544}O_2$ (Ningbo FuLi Battery Materials Technology Co., Ltd) powder and MCMB (Shenzhen BTR Nanotechnology Co., Ltd) powder were commercial. The CR2025 coin-type $Li_{1.144}Ni_{0.136}Co_{0.136}Mn_{0.544}O_2$/Li cells were fabricated to evaluate the effects of phosphite-based additives on the electrochemical performance of LIBs at 4.8 V. The preparation processes of $Li_{1.144}Ni_{0.136}Co_{0.136}Mn_{0.544}O_2$ electrodes and MCMB electrodes are presented in Fig. S1.†

2.2 Measurements

The ionic conductivity of electrolytes was measured using a conductivity meter (DDS-307A, INESA) at room temperature. The electrochemical performances of $Li_{1.144}Ni_{0.136}Co_{0.136}Mn_{0.544}O_2$/Li batteries and MCMB/Li batteries were assessed on a CT2001A tester. In the formation test, the $Li_{1.144}Ni_{0.136}Co_{0.136}Mn_{0.544}O_2$/Li coin cells were subjected to charge–discharge at 0.1 C 3 times and then at 0.2 C 3 times (2.0–4.8 V). After formation, the $Li_{1.144}Ni_{0.136}Co_{0.136}Mn_{0.544}O_2$/Li cells were aged for 10 h and then were subjected to charge–discharge for 200 cycles at 45 °C. The current is 0.5 C and the voltage is 2.0–4.8 V. The storage test was performed after the formation test and then the $Li_{1.144}Ni_{0.136}Co_{0.136}Mn_{0.544}O_2$/Li coin cells were charged to 4.8 V at 0.2 C. The open-circuit voltage was traced at 45 °C. Electrochemical impedance spectroscopy (EIS) was conducted using a frequency response analyzer (VSP, Bio-Logic SAS) from 100 kHz to 0.01 Hz (impedance amplitude: 10 mV). The composition of disassembled electrodes was identified by X-ray

photoelectron spectroscopy (XPS, ESCALAB 250Xi spectrometer) using Al Kα radiation. The content of the transition metal on the cycled lithium electrode was analyzed by inductively coupled plasma-mass spectroscopy (ICP-MS, IRIS Intrepid II XSP). Nuclear magnetic resonance (NMR) was recorded at 400 MHz (Bruker AVANCE III HD). The electrode morphology was characterized by SEM (S-4800).

2.3 Computations

The computations are presented in Table S1.†

3 Results and discussion

3.1 Theoretical analysis of solvents and additives

The chemical structures of TMSPi, TEP, and TMSPE are presented in Fig. 2(a). TMSPi and TEP are the phosphites that contain trimethylsilyl and ethyl, respectively, while TMSPE is the phosphite with trimethylsilyl and ethyl. Fig. 1 and Table S7† exhibit the calculated highest occupied molecular orbital (HOMO) energies, lowest unoccupied molecular orbital (LUMO) energies, and oxidation potential of electrolyte solvents and phosphite-based additives. The calculated HOMO energies of TMSPi, TMSPE, and TEP are −0.2327, −0.2403, and −0.2555 au, respectively. These results indicate that TMSPi is the easiest to be oxidized among the three phosphite-based additives. At the same time, the calculated oxidation potentials of TMSPi, TMSPE, and TEP are 4.28, 4.41, and 4.73 V, indicating that the lower the potential, the easier it is to be oxidized. Furthermore, three phosphites were comparatively evaluated as an additive for the Li-rich lithium battery under high voltage at 45 °C in the present research.

3.2 Effect of additives on the cell performance

The electrolytes with different additives have the same appearance, as displayed in Fig. 2(b). Fig. 2(c) shows the conductivity of electrolytes with different additives. With the addition of the phosphite-based additives, the conductivity of the electrolytes decreased a little. Among these additives, the electrolyte with TMSPE showed a higher conductivity. Fig. 2(d) shows the initial discharge and charge curves for the $Li_{1.144}Ni_{0.136}Co_{0.136}Mn_{0.544}O_2$/Li cells employing electrolytes with different additives. The initial charge and discharge capacities of the cells with TMSPi, TMSPE, and TEP were 325.5 and 298.1, 328.1 and 298, and 386.7 and 268.1 mA h g⁻¹, respectively (Fig. S3 and Table S8†), and their coulombic efficiencies were 91.6%, 90.8% and 69.3%, respectively. The initial charge capacities of the cells are increased in the presence of TMSPi, TMSPE, and TEP. Such a result may be caused by the oxidability difference of the additives. When the additive is easier to be oxidized, the electrolyte is earlier to be protected.

The cycling performance and coulombic efficiency of $Li_{1.144}Ni_{0.136}Co_{0.136}Mn_{0.544}O_2$/Li cells with different P-based
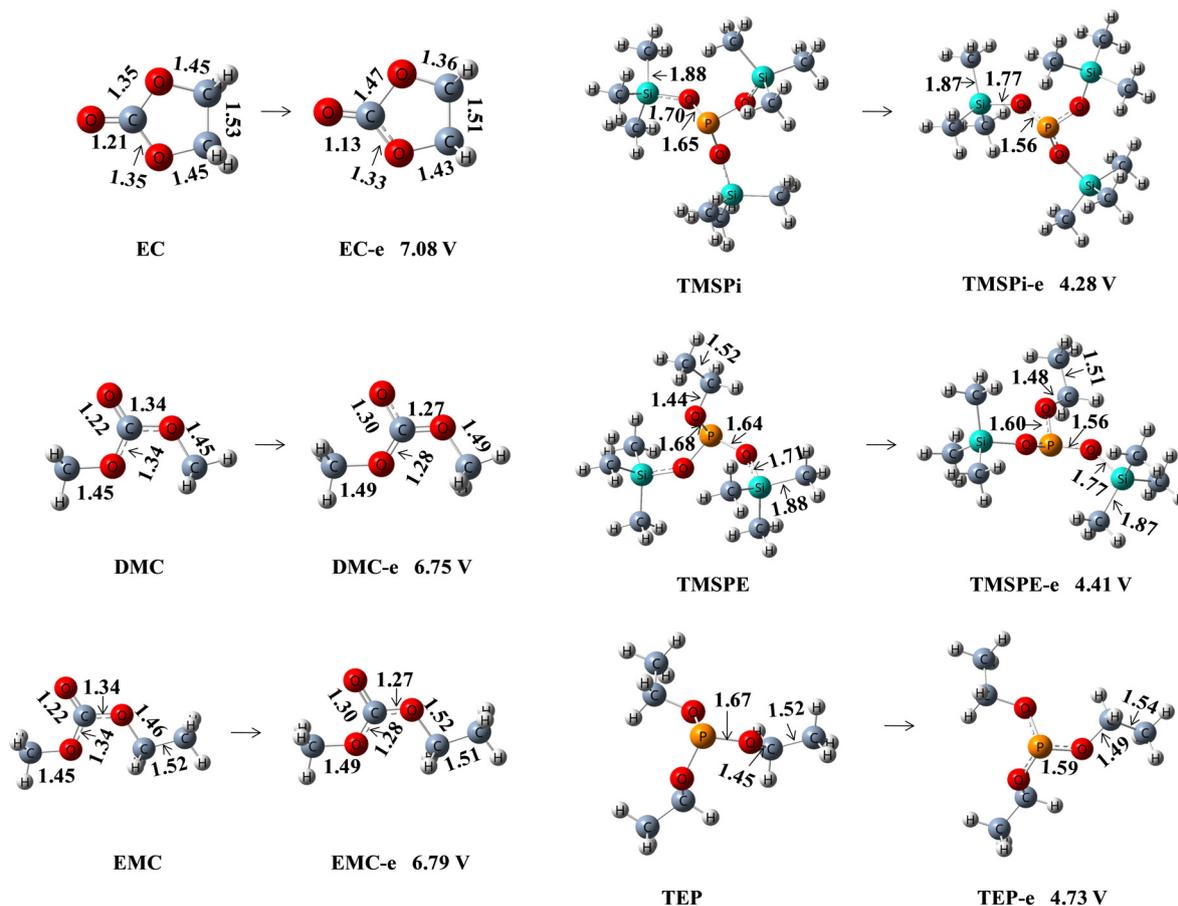
Fig. 1 Optimized structures and calculated oxidation potentials of solvent molecules (EC, DMC, and EMC) and additives (TMSPi, TMSPE, and TEP). The numbers between the bonds represents the bond length (Å).

additives in the electrolyte at 45 °C were tested, as shown in Fig. 2(e and f). Considering the effects of additives on the electrochemical activity of the Li-rich based LIBs, the optimal concentrations of TMSP, TMSPi, TMSPE and TEP were found to be 0.5, 0.5, 0.5 and 3.0 wt% in the electrolyte, respectively (Fig. S4 and S5 and Table S8†). As shown in Fig. S6,† TMSPi shows a better performance than TMSP, which is in accordance with the literature.[26] In order to compare the influence of phosphite on the Li-rich based LIBs, TMSPi, TMSPE, and TEP are separated (Fig. 2(e)). Among these phosphite compounds, TMSPE shows the best performance at 45 °C. The discharge capacity of the cells at the first cycle with TMSPi was 299 mA h g^{-1} and with TMSPE was 297.6 mA h g^{-1}, but 275.2 mA h g^{-1} for TEP. After 200 cycles, the discharge capacity of the battery with TMSPi was 111 mA h g^{-1} and TMSPE was 151.7 mA h g^{-1}, whereas the discharge capacity obtained for the cell with TEP was only 74.1 mA h g^{-1}. As such, the capacity retentions were 37.2%, 50.9%, and 26.9% for cells with TMSPi, TMSPE and TEP, respectively. When charged to 4.8 V, the coulombic efficiency of the cells was more stable during the cycles due to the addition of TMSPE into the electrolyte, as shown in Fig. 2(f).

Fig. 2(g) shows the rate performance of the cells with and without phosphite-based additives. It can be found that the cell cycled without and with additives delivered a similar discharge capacity at a low current density (0.2 C). However, the gap of discharge capacity becomes more and more obvious with the increase of current density (>0.5 C). When the current rate was increased to 3.0 C, the discharge capacity of the cells with TMSPi-containing, TMSPE-containing, and TEP-containing electrolytes remained at 172.5, 189, and 128.5 mA h g^{-1}, respectively, while that of the cell with the additive-free electrolyte was dropped to 121 mA h g^{-1}. The cells with TMSPE show the best rate performance compared with the other two phosphite-based additives and bare electrolytes. This may be contributed to the CEI film produced by TMSPE with the lowest impedance (Fig. 3(a and b)).

Fig. 3(a and b) show the EIS results of the Li$_{1.144}$Ni$_{0.136}$Co$_{0.136}$Mn$_{0.544}$O$_2$/Li cells with different additives after the first cycle and 200th cycle. From Fig. 3(a), the interfacial impedance of the cell with TEP was larger than that with other two additives (TMSPi, TMSPE) after the first cycle. With longer cycling (Fig. 3(b)), the cell without additive exhibited the largest increase in the interfacial impedance compared to the cells with phosphite-based additives. Fig. 3(c) and (d) show the equivalent circuit model that is used to analysis the EIS spectra (R_e is the bulk resistance, R_s is interfacial reaction resistance, and R_{ct} is the charge transfer resistance)[23] and the

© 2025 The Author(s). Published by the Royal Society of Chemistry

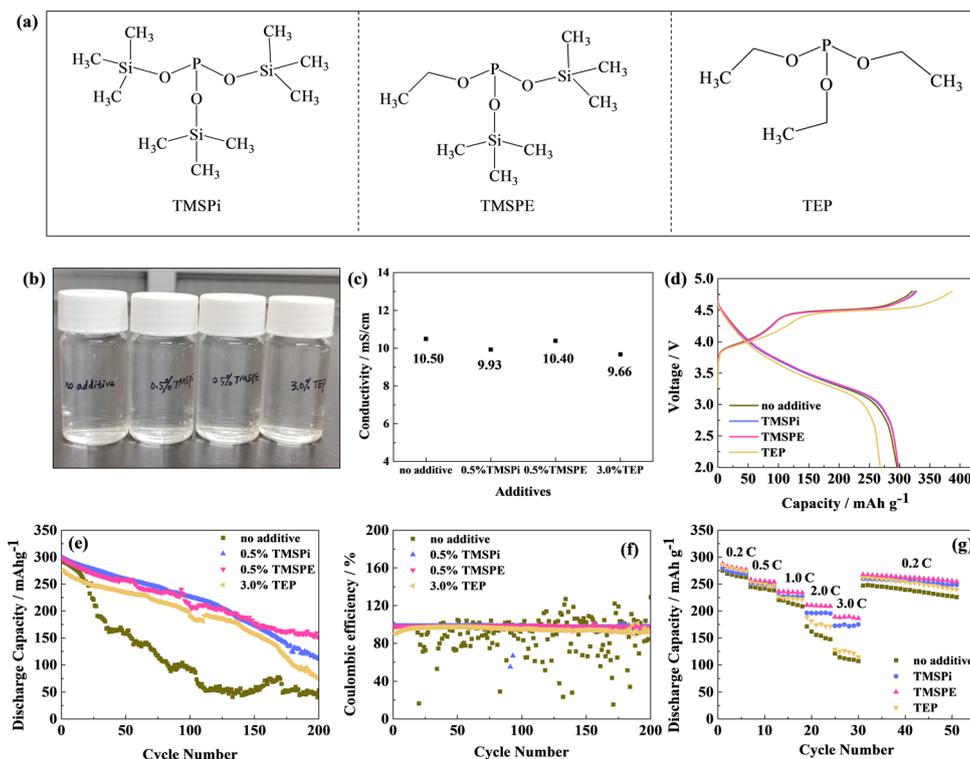*RSC Appl. Interfaces*, 2025, **2**, 251–260 | **253**

Fig. 2 (a) Chemical structures of TMSPi, TMSPE, and TEP; (b) the photograph of the electrolytes with different additives; (c) conductivity of electrolytes with different additives; (d) the initial charge–discharge curve performance of $Li_{1.144}Ni_{0.136}Co_{0.136}Mn_{0.544}O_2$/Li cells with different additives; (e) cycling performance and (f) coulombic efficiency of $Li_{1.144}Ni_{0.136}Co_{0.136}Mn_{0.544}O_2$/Li cells with electrolytes in the different additives at 45 °C; (g) rate performance of $Li_{1.144}Ni_{0.136}Co_{0.136}Mn_{0.544}O_2$/Li cells in the electrolyte with different additives. The test voltage is 2.0–4.8 V (d–g).
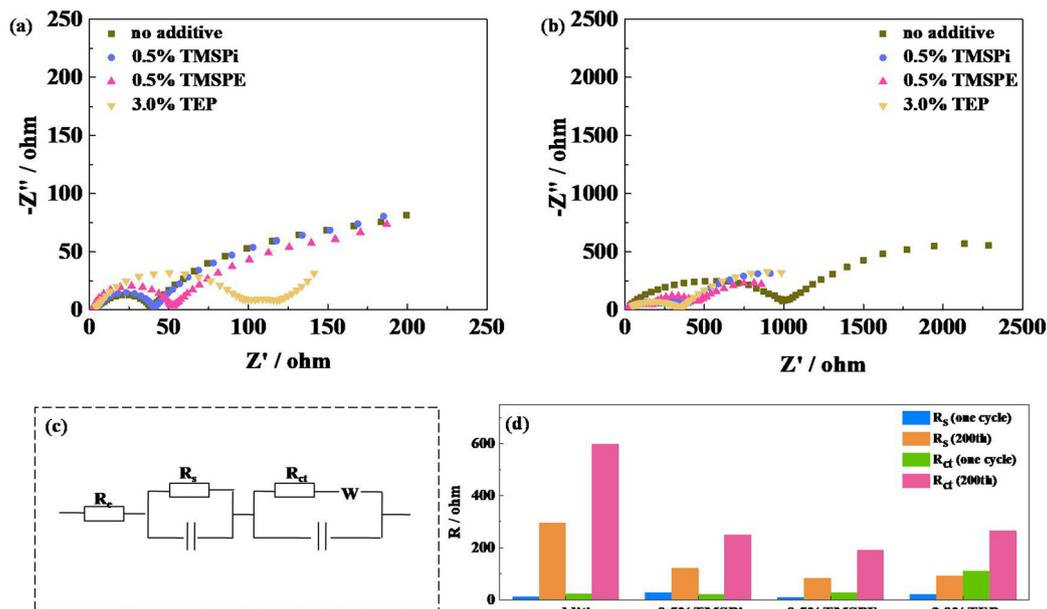

Fig. 3 Electrochemical impedance spectra of $Li_{1.144}Ni_{0.136}Co_{0.136}Mn_{0.544}O_2$/Li cells with different additive charged to 4.8 V after one cycle (a) and the 200 cycles (b); the equivalent circuit model used to analysis the EIS spectra (c) and the fitting result of Rs and Rct of $Li_{1.144}Ni_{0.136}Co_{0.136}Mn_{0.544}O_2$/Li cells with electrolytes in the different additives (d).

fitting results. After 200 cycles, the cell with TMSPE additive exhibited smaller impedance compared with the cells with TMSPi and TEP and without additive. These results indicate that the electrolyte in the presence of TMSPE reduced the impedance of the cell surface film more, which enhanced the Li-rich-based LIB cycling performance.

To further investigate the effect of the phosphite-based additives on the Li-rich electrode at 4.8 V, XPS analysis of the electrodes was carried out after 200 cycles. Fig. 4 shows the C 1s, O 1s, F 1s, P 2p, and Si 2p spectra obtained from XPS analysis of the cycled $Li_{1.144}Ni_{0.136}Co_{0.136}Mn_{0.544}O_2$ electrode. From Fig. 4(a) (C 1s spectra), five peaks located at 284.8 eV (corresponding to C–C), 285.7 eV (corresponding to C–H), 286.6 eV (corresponding to C–O), 288.9 eV (corresponding to C=O) and 290.7 eV (corresponding to C–F) are observed.[38] The peak intensities are different on the cycled cathode surface in the additive-containing electrolyte, suggesting that the decomposition products of three phosphite-based additives are different. The stronger peaks for C–F and C–H of the cycled electrode in the TMSPE-containing electrolyte than that in TMSPi-containing and TEP-containing electrolyte indicate that a thinner film was formed on the cycled cathode surface in the TMSPE-containing electrolyte. The peaks located at 529.8 eV, 531.5 eV, 532.5 eV, and 534.0 eV correspond to Me–O, Li_2CO_3, C=O, and C–O, respectively.[20,39] The peaks for Me–O of the cycled electrode in the TMSPE-containing electrolyte were stronger than those in TMSPi-containing and TEP-containing electrolyte, showing that a thinner film was formed on the surface of the Li-rich electrode cycled in the TMSPE-containing electrolyte. The peaks for Li_2CO_3 of the cycled electrodes in the TEP-containing electrolyte were weaker than that in the TMSPi-containing and TMSPE-containing electrolytes, indicating that less Li_2CO_3 can be formed on the surface of the Li-rich electrolyte cycled in TEP-containing electrolyte. These results declare that the presence of TEP can reduce the Li_2CO_3 formation. When active oxygen existed in the $Li_{1.144}Ni_{0.136}Co_{0.136}Mn_{0.544}O_2$ cathode, the Li_2CO_3 was easily formed. An interaction might be existing between TEP and active oxygen.

Fig. 4(c) shows the F 1s spectra. Three peaks located at 685.2 eV (correspond to LiF), 686.8 eV (correspond to $Li_xPO_yF_z$), and 687.9 eV (correspond to PVDF) are observed, respectively.[40,41] The weaker LiF peaks of the cells with TMPSE-containing additives mean that LiF with a low concentration was coated on the surface of the cathode electrode with the TMSPE-based electrolyte. Less LiF can decrease the interfacial impedance of the cell. The stronger peaks for C–F of the cycled electrode in the TMSPE-containing electrolyte indicate that a thinner film was formed on the cycled cathode surface in the TMSPE-containing electrolyte. The lower $Li_xPO_yF_z$ peak means that salt decomposition in the electrolyte is weaker. Two peaks located at 136.7 eV and 134.1 eV, which correspond to Li_xPF_y and Li_xPOF_y,[42] are observed in the P 2p spectra, as shown in Fig. 4(d). The decomposition of $LiPF_6$ can form LiP_xF_y species $(PF_6^- + ne^- + nLi^+ \rightarrow LiF + Li_xPF_y)$.[38,43] The intensities of Li_xPF_y are weaker in the presence of TMSPE relative to that of the cell with TMSPi and TEP. This result indicates that the addition of TMSPE further prevented the decomposition of $LiPF_6$ under high-voltage conditions. Additional elemental Si was detected in the electrode with the TMSPi and TMSPE additive (Fig. 4(e)), which implies that TMSPi and TMSPE participated in the formation of the film and formed Si-containing species in the cathode electrolyte film.[38,44]

In addition, the Co 2p, Mn 2p, and Ni 2p XPS spectra of the cycled $Li_{1.144}Ni_{0.136}Co_{0.136}Mn_{0.544}O_2$ electrodes with different additives are also presented, as shown in Fig. 5. In

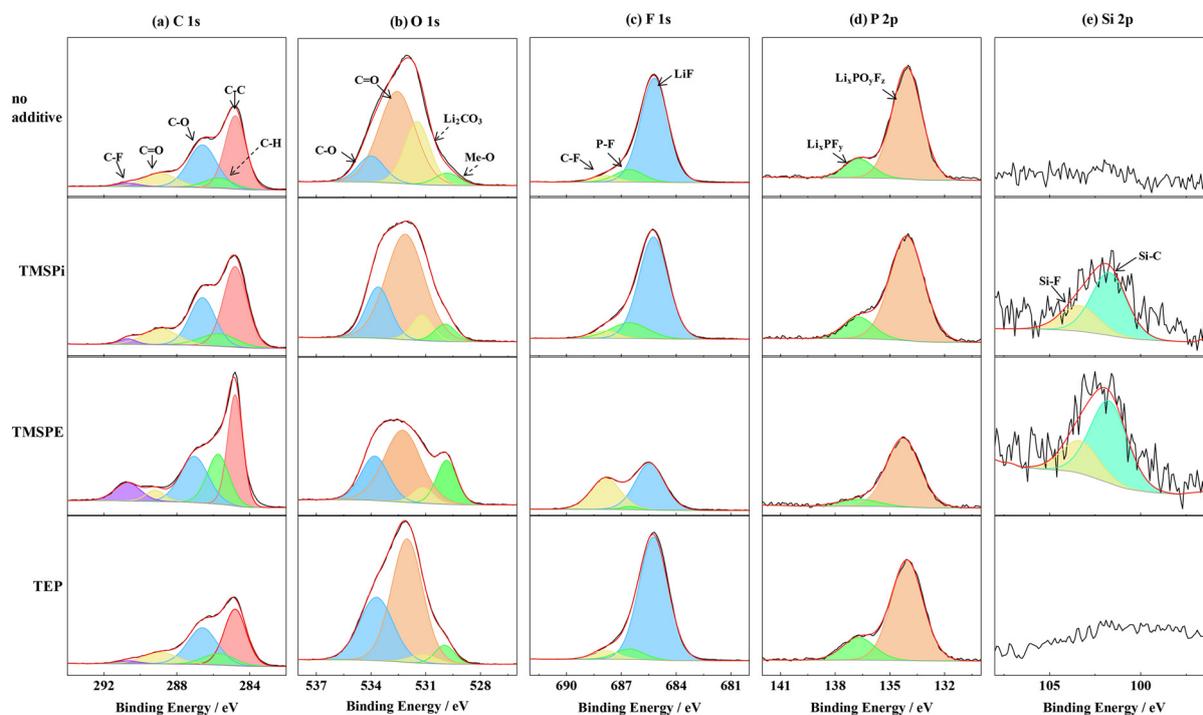**Fig. 4** C 1s (a), O 1s (b), F 1s (c), P 2p (d) and Si 2p (e) XPS spectra of the cycled $Li_{1.144}Ni_{0.136}Co_{0.136}Mn_{0.544}O_2$ electrodes placed in the electrolytes with different additives.

© 2025 The Author(s). Published by the Royal Society of Chemistry

RSC Appl. Interfaces, 2025, **2**, 251–260 | **255**

the fresh $Li_{1.144}Ni_{0.136}Co_{0.136}Mn_{0.544}O_2$ electrode, the binding energies at 780.5, 642.6, and 855.1 eV correspond to Co^{3+}, Mn^{4+} and Ni^{2+}, respectively.[45] The chemical valences of Co, Mn, and Ni are +3, +4, and +2. After 200 cycles, the valences of Co, Mn, and Ni are changed. In the Co 2p spectra (Fig. 5(a)), the valence of Co is +4 (780.6 eV).[46] A stronger peak of Co was observed for the cycled electrode in the TMSPE-containing electrolyte, indicating that a thinner film was formed on the cycled cathode surface in the TMSPE-containing electrolyte. In the Mn 2p spectra (Fig. 5(b)), the main valence of Mn is +4.[47] However, an obvious shift was observed on the surface of the cycled electrode in the base electrolyte and TEP-containing electrolyte. This phenomenon indicates that the valence of Mn ions was lowered.[25] In the Ni 2p spectra, the binding energy of Ni $2p_{3/2}$ is composed of three major peaks at 861.6 eV (Ni^{4+}-containing species), 858.3 eV (NiF_2), and 855.7 eV (Ni^{3+}-containing species).[25] The formation of NiF_2 on the cathode is due to the reaction of HF with Ni^{2+} ions during the discharge process ($Ni^{2+} + 2HF \rightarrow NiF_2 + H_2\uparrow$).[25] Compared with other electrodes, the NiF_2 peaks become weaker for the electrode cycled in the electrolyte with TMSPE, confirming that the presence of TMSPE effectively eliminates HF in the electrolyte.

3.3 Effect of additives on the HF elimination

The calculated reaction energies of TMSPi, TMSPE, TEP, and their cations with an HF molecule are shown in Fig. 6 and S7–S10.† The reactions with HF via the P–O bond, Si–O bond and C–O bond cleavages are considered. TMSPi and $TMSPi^+$ with HF could undergo a favorable reaction by the Si–O bond cleavage (Fig. S7†). This result is consistent with the literature.[48–50] TMSPE and $TMSPE^+$ with HF also undergo a favorable reaction by the Si–O bond cleavage (Fig. S8 and S9†). TEP with HF undergo a favorable reaction by the C–O bond cleavage and TEP^+ with HF undergo a favorable reaction by the P–O bond cleavage (Fig. S10†). The ΔG values of TMSPi, TMSPE, and TEP with HF are −54.59, −62.33, and −44.69 kJ mol^{-1}, respectively, indicating that TMSPE is the most effective HF elimination additive among the three phosphite-based additives, which is consistent with the analysis results in Fig. 5.

To analyze the precipitate on the lithium electrode, ICP-MS was employed. Fig. 7(a and b) provides the contents of Ni, Co, and Mn, which were deposited on the lithium anode disassembled from $Li_{1.144}Ni_{0.136}Co_{0.136}Mn_{0.544}O_2/Li$ cells. Fig. 7(a) shows the photographs of the cycled lithium electrodes disassembled from $Li_{1.144}Ni_{0.136}Co_{0.136}Mn_{0.544}O_2/Li$ cells with different electrolytes. The surface of the lithium electrode without additives was covered with a lot of precipitates. These precipitations might be the deposition of the transition metal that dissolved from the $Li_{1.144}Ni_{0.136}Co_{0.136}Mn_{0.544}O_2$ electrode during cycling. As shown in Fig. 7(b), the contents of Ni, Co, and Mn that are deposited on the lithium electrodes are lower in the electrolyte with phosphite-based additives than that in the electrolyte without additive. ICP-MS results suggest that the addition of phosphite-based additives in the electrolyte can inhibit the dissolution of the transition metal from the cathode material during cycling at a high voltage. Among three additives, TMSPE exhibited the strongest ability to inhibit the dissolution of the transition metal from the cathode material.

Fig. 7(c–f) show the SEM micrographs of the electrodes after cycling without and with different phosphite-based additives in the electrolyte. After cycling in the electrolyte without additives, the $Li_{1.144}Ni_{0.136}Co_{0.136}Mn_{0.544}O_2$ particles cycled without additive were covered with thick deposits, while those cycled with a phosphite-based additive were covered with thinner deposits. It was also detected that the deposits formed by TMSPE were more uniform and stable. This result indicates that the addition of TMSPE would form more effective CEI films compared to the other two additives (TMSPi and TEP). The addition of TMSPE would effectively prevent the erosion of the electrolytes at a high voltage under 45 °C and enhance cell performance.

In order to verify the effect of TMSPE on the removal of HF from the electrolyte, 1000 ppm water was added to the electrolytes with and without additives. Then, the electrolytes were stored at 25 °C for 24 h. Fig. 8(a and b) show the ^{19}F NMR spectra of the electrolytes with and without TMSPE after storage. The peak at 188 ppm corresponds to HF.[51] After storage, HF can easily be identified in the electrolyte without additives (Fig. 8(a)), but hardly be identified when TMSPE is
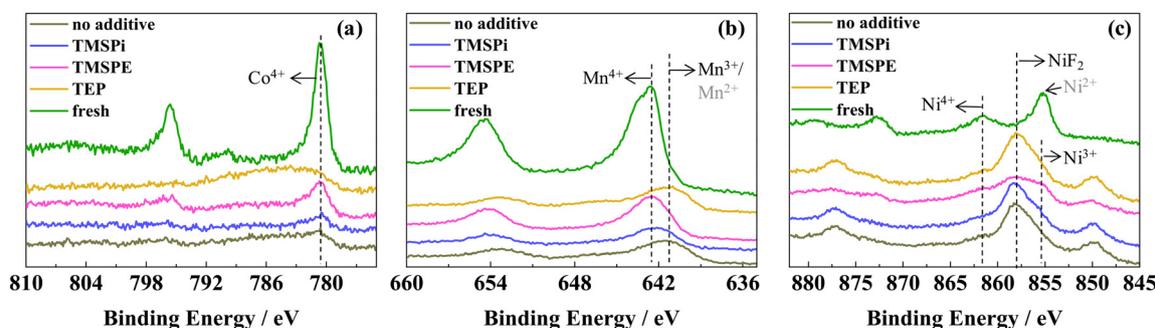

Fig. 5 The Co 2p (a), Mn 2p (b) and Ni 2p (c) XPS spectra of the cycled $Li_{1.144}Ni_{0.136}Co_{0.136}Mn_{0.544}O_2$ electrodes placed in the electrolytes with different additives.
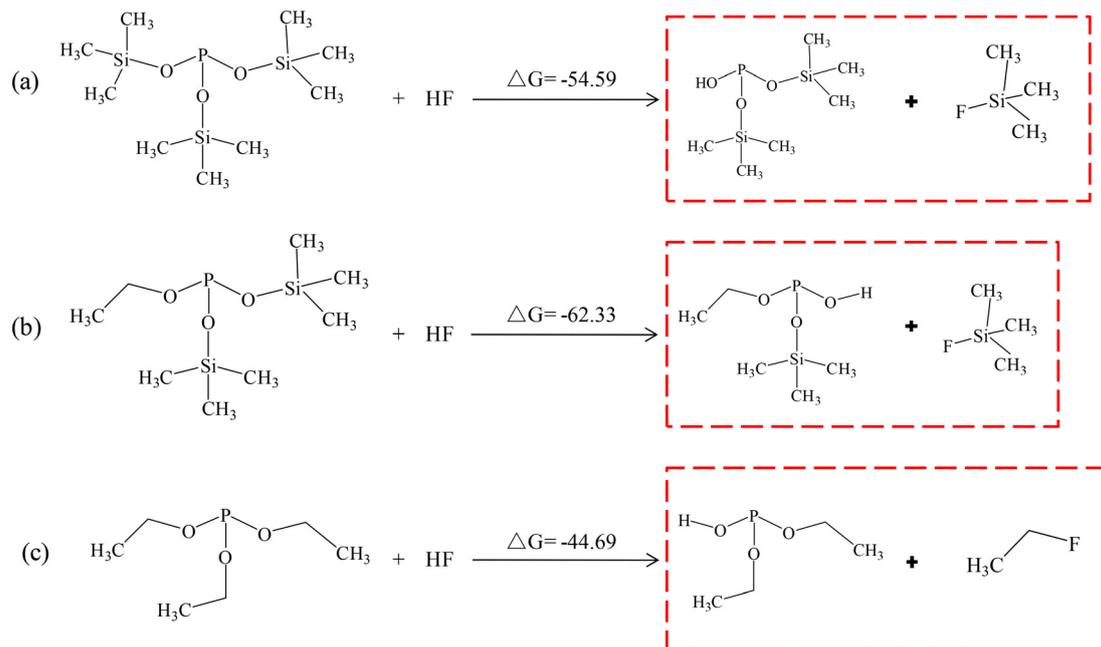
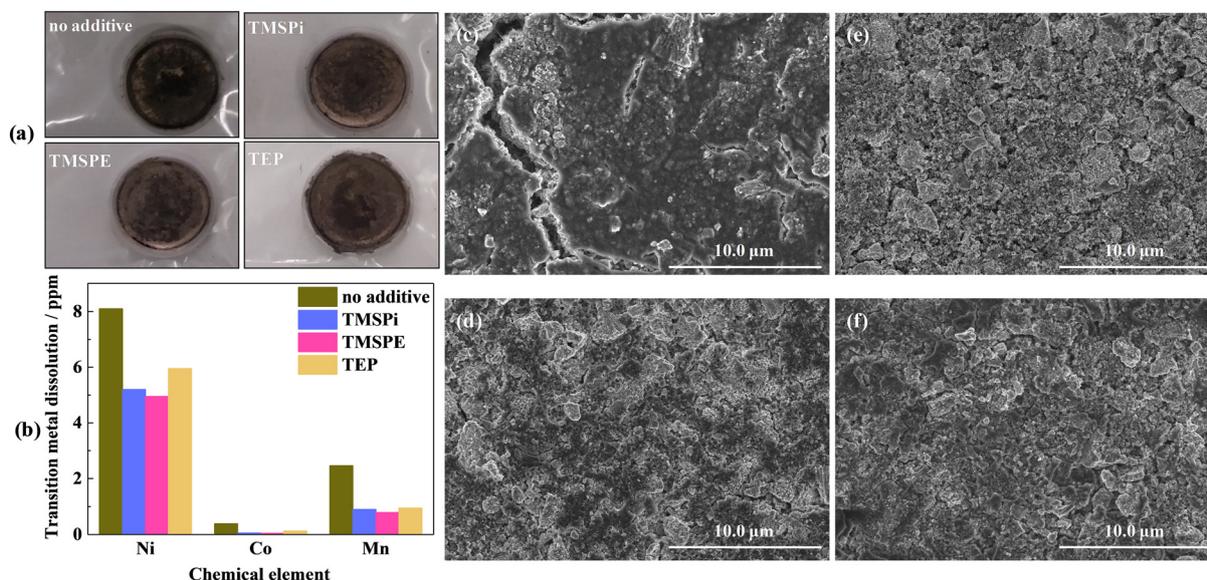**Fig. 6** Reaction energies (ΔG in kJ mol^{-1}) of (a) TMSPi, (b) TMSPE, and (c) TEP with a HF molecule.

Fig. 7 (a) Photographs of the cycled lithium electrodes disassembled from $Li_{1.144}Ni_{0.136}Co_{0.136}Mn_{0.544}O_2$/Li cells with different electrolytes; (b) contents of transition metal elements deposited on lithium electrodes from cycled $Li_{1.144}Ni_{0.136}Co_{0.136}Mn_{0.544}O_2$/Li cells in different electrolytes; SEM micrographs of cycled $Li_{1.144}Ni_{0.136}Co_{0.136}Mn_{0.544}O_2$ electrode without additive (c), with TMSPi (d), with TMSPE (e) and with TEP (f) after 200 cycles.

added to the electrolyte (Fig. 8(b)). It is obvious that HF can be effectively eliminated by adding TMSPE. Fig. S11† shows the ^{19}F NMR spectra of the electrolytes with different additives after storage. It is found that TMSPE is the most effective HF elimination additive among the three phosphite-based additives from the ^{19}F NMR spectra. Fig. 8(c) and S12† show the combination energies between HF and solvents (EC, DMC, and EMC) and phosphite-based additives, which had been used to understand the contribution of TMSPE to eliminate the negative effects of HF. Fig. 8(c) shows that the combination energies of EC (-37.21 kJ mol^{-1}), DMC (-34.57 kJ mol^{-1}) and EMC (-35.16 kJ mol^{-1}) with HF are higher than that of TMSPE (-44.25 kJ mol^{-1}), suggesting that TMSPE will preferentially interact with HF compared to the solvents. Among the three phosphite-based additives, TMSPE also
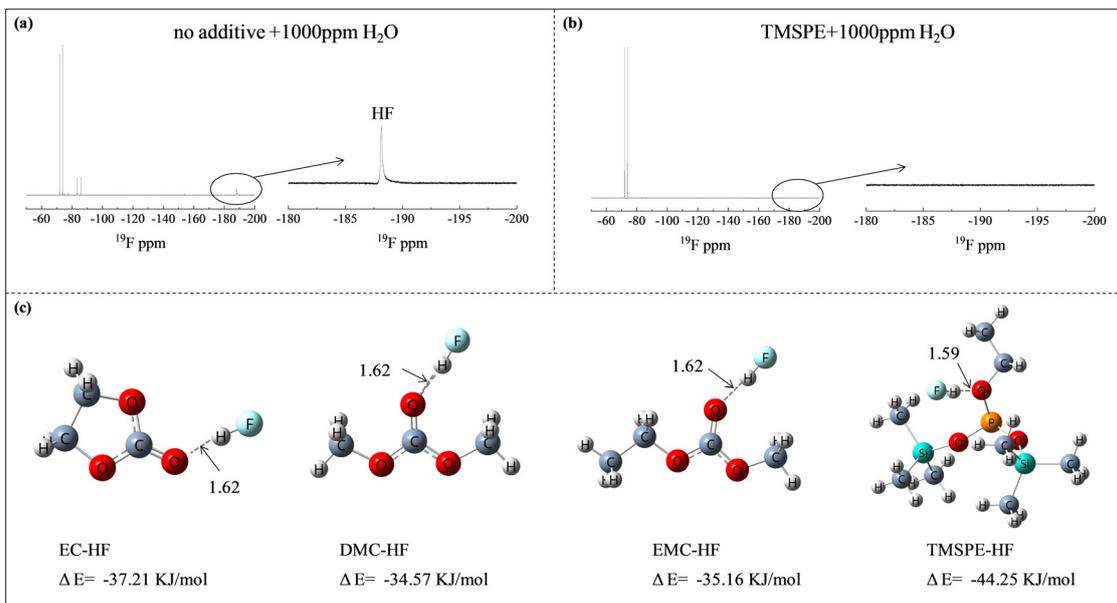
Fig. 8 (a and b) ^{19}F NMR spectra of the electrolytes with and without adding 0.5% TMSPE after storage under 25 °C for 24 h; (c) optimized structures and the relative combination energies (ΔE, kJ mol^{-1}) between HF and solvents or an electrolyte additive: DMC/EC/EMC/TMSPE-HF.

exhibited the preferential ability to interact with HF (Fig. S12†).

Fig. S13† shows the results of the storage performance of $Li_{1.144}Ni_{0.136}Co_{0.136}Mn_{0.544}O_2$/Li at 45 °C with TMSPi, TMSPE, and TEP. In the curves of cells without additives, four platforms are observed. The plateaus at 4.5–4.0 V, 4.0–3.7 V and 3.7–3.0 V are attributed to the reduction of $Co^{4+} \rightarrow Co^{3+}$ (point a to b), $Ni^{4+} \rightarrow Ni^{2+}$ (point b to c), and $Mn^{4+} \rightarrow Mn^{3+}$ (point c to d), respectively, and the point d to e is attributed to the formation of new compounds.[52,53] After storage for 20 days, the voltage of $Li_{1.144}Ni_{0.136}Co_{0.136}Mn_{0.5446}O_2$/Li cell in the electrolyte without additives decreased more than those of cells in the phosphite-containing electrolytes. These results indicate that the addition of phosphite additives can suppress the self-discharge of the charged $Li_{1.144}Ni_{0.136}$-$Co_{0.136}Mn_{0.544}O_2$ effectively. In the phosphite-containing electrolyte, a protective CEI film can be formed on the surface of $Li_{1.144}Ni_{0.136}Co_{0.136}Mn_{0.544}O_2$ due to the preferential oxidation of these phosphite-based additives,[53] which can separate the $Li_{1.144}Ni_{0.136}Co_{0.136}Mn_{0.544}O_2$ cathode from direct contact with the electrolyte and thus suppress the self-discharge of the charged $Li_{1.144}Ni_{0.136}Co_{0.136}Mn_{0.544}O_2$. The CEI film formed by TMSPE is more stable than that of TMSPi or TEP.

Considering the positive effect of TMSPE on the anode, we also tested the performance of mesocarbon microbead (MCMB)/Li cells. Fig. S14† shows the cycling performance of MCMB/Li cells with electrolytes in the different additives. It can be seen that the addition of TMSPE can improve the electrochemical performance of MCMB/Li cells.

Based on the aforesaid results from EIS, XPS spectra, ICP, SEM measurements and NMR, we conclude that TMSPE showed the best electrochemical performance among the

three phosphite-based additives. These improvements might be attributed to the functional groups in TMSPE. The trimethylsilyl and ethyl functional groups in TMSPE can form Si-containing species CEI films and provide lower interfacial impedance, stronger HF elimination, transition metal dissolution inhibition and lower Li_2CO_3 content. The interaction of two functional groups in TMSPE makes its CEI have the best properties among the three additives, and then enhance the cell electrochemical performance.

Conclusions

In summary, we comparatively evaluated TMSPi, TMSPE, and TEP as additives for high temperature application of a Li-rich lithium battery at a high voltage. The capacity retentions were 37.2%, 50.9% and 26.9% for cells with TMSPi, TMSPE and TEP after 200 charge–discharge cycles at 45 °C. When charged to 3 C, the discharge capacity of cells with TMSPE reached 189 mA h g^{-1}, while that of cells with TMSPi and TEP was 172.5 mA h g^{-1} and 128.5 mA h g^{-1}, respectively. In the electrochemical tests, TMSPE showed the best performance between the three additives. The results from EIS, XPS spectra, ICP, SEM measurements and NMR indicate that the CEI film generated by TMSPE is thinner and more stable among the three additives. With the help of this CEI film, the electrochemical performance of cells cycled in TMSPE showed the best performance, which might be attributed to the interaction of functional groups (trimethylsilyl and ethyl) in TMSPE. The trimethylsilyl and ethyl functional groups in TMSPE can form Si-containing species CEI films and provided lower interfacial impedance, stronger HF elimination, and transition metal dissolution inhibition. The interaction of functional groups makes

TMSPE have a good oxidation potential, which can effectively inhibit the decomposition of the electrolyte and the change of battery materials. Thus, such a study would provide more reference for the future development of additive diversity.

Data availability

The data supporting this article have been included as part of the ESI.†

Author contributions

Xiangzhen Zheng carried out the experiments and drafted the manuscript. Tao Huang contributed to the electrochemistry analysis. Ying Pan conducted the computations. Yongwei Chen contributed to the characterization testing. Mingdeng Wei provided guidance on data interpretation and edited the manuscript. Maoxiang Wu supervised the project and edited the manuscript.

Conflicts of interest

There are no conflicts to declare.

Acknowledgements

Notes and references

1 K. Kim, D. Hwang, S. Kim, S. O. Park, H. Cha, Y.-S. Lee, J. Cho, S. K. Kwak and N.-S. Choi, *Adv. Energy Mater.*, 2020, 2000012.

2 R. Wang, B. Weng, A. Mahadevegowda, I. Temprano, H. Wang, Z. He, C. Ducati, Y. G. Xiao, C. P. Grey and M. F. L. De Volder, *Adv. Energy Mater.*, 2024, **14**, 2401097.

3 H. Wu, W. F. Feng, M. Armand, Z. B. Zhou and H. Zhang, *ACS Appl. Mater. Interfaces*, 2024, **16**, 48748–48756.

4 S. Yang, G. Li, X. Lin, C. Mo, X. Zhou, L. Quan, K. Zhou, S. Li, H. Wang and W. Li, *J. Energy Chem.*, 2023, **78**, 80–90.

5 W. Y. Wu, Y. Bai, X. R. Wang and C. Wu, *Chin. Chem. Lett.*, 2021, **32**, 1309–1315.

6 J. N. Liu, S. C. He, S. Q. Liu, S. Q. Wang and J. J. Zhang, *J. Mater. Chem. A*, 2022, **10**, 22929–22954.

7 J. Zhao, X. Zhang, Y. Liang, Z. Han, S. Liu, W. Chu and H. Yu, *ACS Energy Lett.*, 2021, **6**, 2552–2564.

8 X. W. Lan, S. S. Yang, T. Meng, C. S. Zhang and X. L. Hu, *Adv. Energy Mater.*, 2023, **13**, 2203449.

9 X. He, Y. Li, W. Wang, X. Zeng, H. Hu, H. Li, W. Fan, C. Fan, J. Cai, Z. Ma and J. Nan, *J. Energy Chem.*, 2023, **80**, 10–22.

10 Y.-X. Huang, Y.-X. Xie, M.-L. Sun, H. Chen, P. Dai, S.-S. Liu, C.-Y. Ouyang, C.-Y. Liu, B.-B. Hu, S.-J. Liao, L. Huang and S.-G. Sun, *ACS Sustainable Chem. Eng.*, 2023, **11**, 3760–3768.

11 J. P. Mu, X. H. Li, R. He, L. J. Sun, X. Bai, L. H. Zhang, X. Zhang, Z. F. Liu, J. Gao and A. J. Wei, *Acta Mater.*, 2024, **278**, 120252.

12 N. Gogoi, E. Bowall, R. Lundström, N. Mozhzhukhina, G. Hernández, P. Broqvist and E. J. Berg, *Chem. Mater.*, 2022, **34**, 3831–3838.

13 S. M. Chen, G. R. Zheng, X. M. Yao, J. L. Xiao, W. G. Zhao, K. Li, J. J. Fang, Z. N. Jiang, Y. X. Huang, Y. C. Ji, Y. Kang, Z. W. Yin, M. Zhang, F. Pan and L. Y. Yang, *Nano*, 2024, **18**, 6600–6611.

14 Y. X. Li, W. K. Li, R. Shimizu, D. Y. Cheng, H. N. Nguyen, J. Paulsen, S. Kumakura, M. H. Zhang and Y. S. Meng, *Adv. Energy Mater.*, 2022, **12**, 2103033.

15 J. N. Li, J. Z. Yang, Z. Q. Ji, M. Su, H. J. Li, Y. C. Wu, X. Su and Z. C. Zhang, *Adv. Energy Mater.*, 2023, **13**, 2301422.

16 J. Zhang, J. Wang, J. Yang and Y. NuLi, *Electrochim. Acta*, 2014, **117**, 99–104.

17 D. S. Lu, J. He, Y. J. Qiu, J. Zhu, M. Y. Zhang and Y. P. Cai, *ACS Appl. Energy Mater.*, 2022, **5**, 13600–13609.

18 H. J. Zhao, Y. X. Qian, S. G. Hu, G. F. Luo, C. X. Nie, P. Q. Qiu, Y. Y. Kang, H. Wang, Y. L. Chu, Q. R. Wang, J. Wang, H. Y. Shao, K. Xu and Y. H. Deng, *ACS Appl. Mater. Interfaces*, 2021, **13**, 29676–29690.

19 H. Rong, M. Xu, B. Xie, W. Huang, X. Liao, L. Xing and W. Li, *J. Power Sources*, 2015, **274**, 1155–1161.

20 H. Rong, M. Xu, L. Xing and W. Li, *J. Power Sources*, 2014, **261**, 148–155.

21 L. Xia, Y. Xia and Z. Liu, *J. Power Sources*, 2015, **278**, 190–196.

22 F. B. Ajdari, A. F. Zonouz, A. Heydari, H. S. Mehrabani, M. Shakourian-Fard, G. Kamath, F. Ghasemi and M. Kahrizi, *J. Phys. Chem. C*, 2023, **127**, 8195–8207.

23 T. Huang, X. Z. Zheng, G. F. Fang, Y. Pan, W. G. Wang and M. X. Wu, *RSC Adv.*, 2017, **7**, 47775–47780.

24 B. Koo, J. Lee, Y. Lee, J. K. Kim and N.-S. Choi, *Electrochim. Acta*, 2015, **173**, 750–756.

25 J.-G. Han, S. J. Lee, J. Lee, J.-S. Kim, K. T. Lee and N.-S. Choi, *ACS Appl. Mater. Interfaces*, 2015, **7**, 8319–8329.

26 S. Mai, M. Xu, X. Liao, J. Hu, H. Lin, L. Xing, Y. Liao, X. Li and W. Li, *Electrochim. Acta*, 2014, **147**, 565–571.

27 Z. D. Li, Y. C. Zhang, H. F. Xiang, X. H. Ma, Q. F. Yuan, Q. S. Wang and C. H. Chen, *J. Power Sources*, 2013, **240**, 471–475.

28 W. Tu, P. Xia, X. Zheng, C. Ye, M. Xu and W. Li, *J. Power Sources*, 2017, **341**, 348–356.

29 J. Song, F. Ning, Y. Zuo, A. Li, H. Wang, K. Zhang, T. Yang, Y. Yang, C. Gao, W. Xiao, Z. Jiang, T. Chen, G. Feng and D. Xia, *Adv. Mater.*, 2023, **35**, 2208726.

30 X. T. Yan, X. Y. Zhou, C. W. Zhu, W. J. Huang and Y. J. Zhao, *J. Mater. Chem. A*, 2024, **12**, 3722–3733.

31 X. Li, Y. Qiao, S. Guo, Z. Xu, H. Zhu, X. Zhang, Y. Yuan, P. He, M. Ishida and H. Zhou, *Adv. Mater.*, 2018, **30**, 1705197.

32 P. Yan, J. Zheng, Z.-K. Tang, A. Devaraj, G. Chen, K. Amine, J.-G. Zhang, L.-M. Liu and C. Wang, *Nat. Nanotechnol.*, 2019, **14**, 602–608.

33 W. He, W. Guo, H. Wu, L. Lin, Q. Liu, X. Han, Q. Xie, P. Liu, H. Zheng, L. Wang, X. Yu and D.-L. Peng, *Adv. Mater.*, 2021, **33**, 2005937.

34 L. C. Zeng, H. Y. Liang, B. Qiu, Z. P. Shi, S. J. Cheng, K. X. Shi, Q. B. Liu and Z. P. Liu, *Adv. Funct. Mater.*, 2023, **33**, 2213260.

35 T. Jenkins, J. A. Alarco, B. Cowie and I. D. R. Mackinnon, *J. Mater. Chem. A*, 2022, **10**, 24487–24509.

36 B. Jiang, H. Li, B. Luo, L. H. Liu, L. H. Chu, Q. B. Zhang and M. C. Li, *Chin. Chem. Lett.*, 2024, **35**, 108649.

37 Y.-X. Li, X. Ding, F. Chen, K. Cao and C.-H. Chen, *J. Power Sources*, 2022, **551**, 232175.

38 C. Ye, W. Tu, L. Yin, Q. Zheng, C. Wang, Y. Zhong, Y. Zhang, Q. Huang, K. Xu and W. Li, *J. Mater. Chem. A*, 2018, **6**, 17642–17652.

39 Z. Wang, L. Xing, J. Li, M. Xu and W. Li, *J. Power Sources*, 2016, **307**, 587–592.

40 J. Li, L. Xing, R. Zhang, M. Chen, Z. Wang, M. Xu and W. Li, *J. Power Sources*, 2015, **285**, 360–365.

41 T. Deng, X. Fan, L. Cao, J. Chen, S. Hou, X. Ji, L. Chen, S. Li, X. Zhou, E. Hu, D. Su, X.-Q. Yang and C. Wang, *Joule*, 2019, **3**, 2550–2564.

42 G. Xu, Z. Liu, C. Zhang, G. Cui and L. Chen, *J. Mater. Chem. A*, 2015, **3**, 4092–4123.

43 D. Aurbach, E. Zinigrad, Y. Cohen and H. Teller, *Solid State Ionics*, 2002, **148**, 405–416.

44 R. Ofer, S. Zachi, H. Rika and E.-E. Yair, *J. Electrochem. Soc.*, 2010, **157**, H281–H286.

45 B. Song, M. O. Lai, Z. Liu, H. Liu and L. Lu, *J. Mater. Chem. A*, 2013, **1**, 9954–9965.

46 Y. Zhu, X. Luo, M. Xu, L. Zhang, L. Yu, W. Fan and W. Li, *J. Power Sources*, 2016, **317**, 65–73.

47 G. Xu, C. Pang, B. Chen, J. Ma, X. Wang, J. Chai, Q. Wang, W. An, X. Zhou, G. Cui and L. Chen, *Adv. Energy Mater.*, 2018, **8**, 1701398.

48 Y.-K. Han, J. Yoo and T. Yim, *Electrochim. Acta*, 2016, **215**, 455–465.

49 D. Y. Kim, H. Park, W. I. Choi, B. Roy, J. Seo, I. Park, J. H. Kim, J. H. Park, Y.-S. Kang and M. Koh, *J. Power Sources*, 2017, **355**, 154–163.

50 Y.-K. Han, J. Yoo and T. Yim, *RSC Adv.*, 2017, **7**, 20049–20056.

51 X. Yang, J. Chen, Q. Zheng, W. Tu, L. Xing, Y. Liao, M. Xu, Q. Huang, G. Cao and W. S. Li, *J. Mater. Chem. A*, 2018, **6**, 16149–16163.

52 J. Li, L. Xing, L. Zhang, L. Yu, W. Fan, M. Xu and W. Li, *J. Power Sources*, 2016, **324**, 17–25.

53 X. Liao, Q. Huang, S. Mai, X. Wang, M. Xu, L. Xing, Y. Liao and W. Li, *J. Power Sources*, 2015, **286**, 551–556.